Indoor Office Wideband MIMO Channel Characteristics at 3.7 GHz

Jae-Joon Park, Heon-Kook Kwon, Hyun-Kyu Chung
Wireless Telecommunications Research Department
Electronics and Telecommunications Research Institute
161, Gajeong-dong, Yuseong-gu, Daejeon, 305-700, Korea
E-mail: {jjpark, hkkwon, hkchung}@etri.re.kr

***Abstract*—In this paper, we present propagation characteristics of the wideband MIMO channel based on indoor measurement. Statistical characterization of the wideband MIMO channel is crucial for the design of wireless mobile broadband communication systems, especially upcoming IMT-Advanced systems. We performed measurement campaign for the indoor office scenario using the Band Exploration and Channel Sounding (BECS) system developed by ETRI with 100 MHz RF bandwidth at 3.7 GHz which is the frequency band for IMT systems. Based on the measured data, we analyze the large-scale (LS) parameters, such as delay spread (DS) and angular spread (AS) of the wideband indoor office scenario. Additionally, we present cross-correlations between the LS parameters and clustering characteristics of multi-path components.**

I. Introduction

For developing new and more efficient wireless communication systems, we need to know the propagation channel widely and exactly. Channel measurements can be used in acquiring measurement data of different kind of wireless propagation channels, such as multiple-input multiple-output (MIMO) channels, indoor and outdoor channels. Using high-resolution parameter estimation methods, channel parameters of the propagating multi-paths, such as delay, angle of departure (AoD) and angle of arrival (AoA) can be extracted from the measurement data, and the estimated channel parameters can be used in developing MIMO channel models.

With constantly growing need of larger capacities, MIMO technology has been extensively studied during the last decades. The use of MIMO can significantly increase the capacity of wireless communication systems, and it would greatly enhance the spectral efficiency of wireless communication systems.

During the last few years commercial wireless local area network (WLAN) products based on the IEEE 802.11n [1] standard, that utilizes MIMO technology, have been introduced by many companies. Recently, IEEE 802.11ac task group (TGac) [2] is targeting above 1 Gbps throughput (VHT: very high throughput) using one or more of the following technologies: high order MIMO (above 4×4), higher bandwidth (above 40 MHz), multi-user MIMO with above 4 access point (AP) antennas and OFDMA. Most probably in the near future also other wireless networks will go towards MIMO technology.

The wireless access networks, e.g. WLAN and worldwide interoperability for microwave access (WiMAX), have become more and more popular and this kind of networks can be found from many places, e.g. airport terminals, shopping malls or cafeterias usually have one or several networks of this kind. As the MIMO products become popular more and more, and as the deployment of the base stations becomes more dense, the need to understand the effects of channel characteristics becomes more important. For this purpose, measurements and analysis of MIMO propagation channel especially in indoor scenarios are needed.

The performance of wireless communication systems highly depends on the channel characteristics, such as large-scale (LS) parameters, including delay spread (DS) and angular spread (AS). Path loss and shadow fading effects are important for coverage prediction and interference analysis and the delay characteristics shows the frequency selectivity of the wideband channel. Moreover, composite AS and AS of each cluster affect the system capacity. Therefore, we present LS parameters, i.e. delay spread, angular spread of arrival (ASA) and angular spread of departure (ASD) based on the measurement data in a typical office. We also present cross-correlations between the LS parameters and clustering characteristics.

This paper organized as follows. In the section II, measurement environment is described. And statistical analysis results of the LS parameters are presented in the section III. Finally, the section IV gives conclusions.

II. Measurement Environment

A. Measurement System

The channel measurement campaign was performed using the channel sounder BECS system [3]. As a time division multiplexing (TDM) based wideband MIMO radio channel sounder, the BECS system is designed for MIMO channel sounding at carrier frequency of 3.7 GHz and 5.2 GHz with 100 MHz bandwidth and 2.3 GHz with 20 MHz bandwidth using 8×8 array antennas. The BECS system uses pseudorandom noise (PN) sounding technique to sequentially transmit multiple PN signals. Multiple receivers then receive the transmitted signal sequentially. The complex channel impulse responses

This work was supported by the IT R&D program of KCC/KCA of Korea, [09911-01104, Wideband Wireless Channel Modeling based on IMT-Advanced]

Fig. 1. 8-elements uniform circular array antenna was used at the TX/RX

(CIRs) are extracted based on the cross-correlation properties between the received signals and the probing PN sequences.

Summary of the BECS system parameters which were used in the measurement campaign is given in Table I. And Fig. 1 shows 8-elements uniform circular array (UCA) antenna with radius of 0.5λ. During the measurement campaign, we used the UCA antenna at both sides of the transmitter (Tx) and the receiver (Rx).

Parameter	Value
Center frequency [GHz]	3.705
Bandwidth [MHz]	100
Tx Power [dBm]	19
Tx/Rx elements	8/8
Code length [chips]	4095
Chip rate [MHz]	100
Channel Sampling rate [MHz]	400

TABLE I
MEASUREMENT SYSTEM PARAMETERS

B. Measurement Scenarios

The indoor measurement campaign was conducted in a typical office of the ETRI, Korea. The site map and the Tx/Rx locations are given in Fig. 2. In the figure, the Tx was located at the center of the office (red point) and the Rx was distributed evenly in the office (blue or green points). Blue and green points denote line of site (LOS) and non-LOS (NLOS) locations, respectively. And arrows indicate the direction of 0°. Fig. 3 shows the photographs of the surroundings of the Tx/Rx when the Rx was located at position 9 (Rx9).

Dimensions of the office are 33m×21m×2.6m (L×W×H). The Tx antenna is 2m high just below the ceiling and the Rx antenna is 1m high considering office workers. The outside walls of the building are largely glass, whereas the inside walls and ceilings are made of reinforced concrete and plaster. As we can see from Fig. 2 and 3, there are many scatterers around the Tx/Rx, such as pillars and steel frames. We measured LOS scenarios at 6 positions (Rx3, Rx4, Rx6, Rx7, Rx10 and Rx12) and NLOS scenarios at 7 positions (Rx1, Rx2, Rx5, Rx8, Rx9, Rx11 and Rx13).

In this scenario, 20 snapshots of CIRs were recorded for the analysis at each Rx location. During the measurement campaign, the Tx and the Rx were fixed stationary except but moving scatterers.

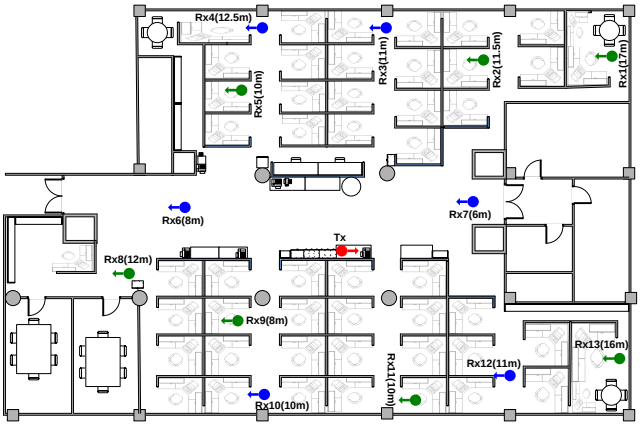

Fig. 2. Indoor measurement campaign - Office scenario

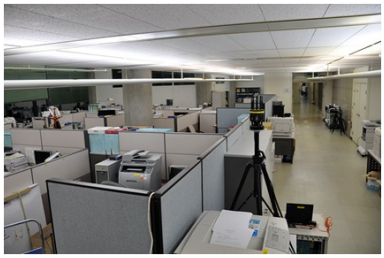

(a) Surrounding of the Tx

(b) Surrounding of the Rx

Fig. 3. Photographs of the indoor office measurement

III. ANALYSIS RESULTS

The BECS system consists of a baseband unit, a RF transceiver unit, a RF Front-end Unit and multiple antennas. The transmitting signals are filtered through a pulse shaping root-raised-cosine (RRC) filter in digital domain. A modulated intermediate frequency (IF) data is downloaded to the Tx digital baseband block and it is fed into high-speed D/A convertor to make analog IF signal. The IF signal is up-converted to RF frequency and then sequentially transmitted through the multiple antennas by selection of RF high power switch. At the receiver side, data is sequentially acquired through whole antenna elements. The RF input is filtered and amplified and feed to high-speed A/D convertor. Down-converted and demodulated I-Q data is saved in the Rx digital baseband block of baseband unit.

The overall system impulse response (SIR) of the BECS

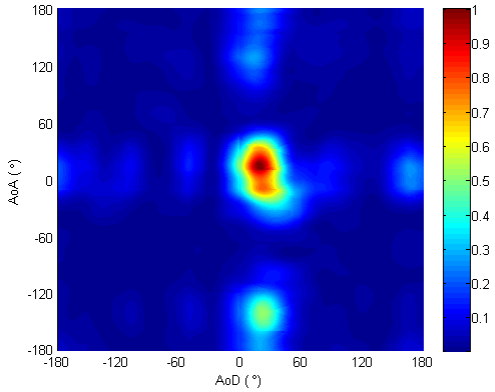

(a) Rx7-LOS

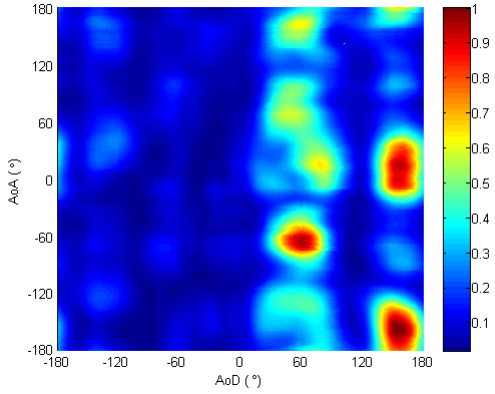

(b) Rx1-NLOS

Fig. 4. Power azimuth spectrum (PAS)

system can be measured by taking a measurement via directly connecting a cable between the RF ports of the Tx and the Rx. Before the measurement campaign, we measured the SIR for the system calibration. After calibrating measured CIRs by using the SIR, we estimate the channel parameters of multi-path components.

The space-alternating generalized expectation-maximization (SAGE) algorithm [4] is an iteration-based algorithm which provides channel parameter estimates approximately equal to the maximum likelihood estimates. In this paper, we use the SAGE algorithm to estimate parameters of multi-paths, such as delays, angles (AoA and AoD) and complex attenuations of 20 propagation multi-paths.

In order to verify whether the measurement campaign was conducted very well and to observe the channel environments, we estimated power azimuth spectrum (PAS) of the received signal by using conventional beamforming method. Fig. 4 displays estimated result of PAS at the Rx1 and the Rx7. From Fig. 4, we could observe that a dominant path having the largest power departs by angle of about 13° and arrives by angle of about 20° in case of LOS. As a result, we confirmed that our measurement campaign was performed well. In case of NLOS, we could also observe that there are many strong

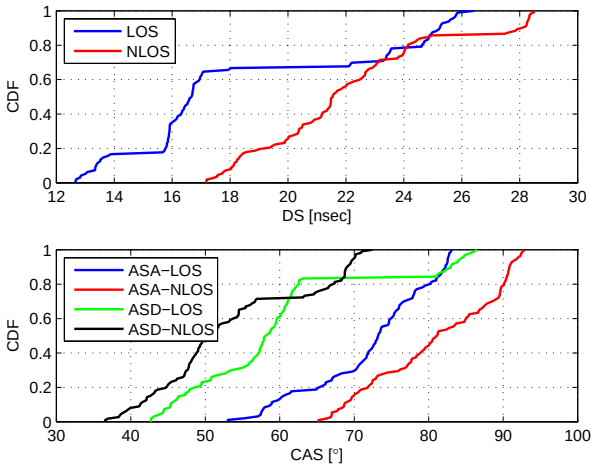

Fig. 5. DS and CAS of the indoor office scenario

scatterers around the Tx/Rx.

Measured CIRs with more than 20 dB dynamic range (maximum peak to noise ratio) were included when we estimated the parameters of multi-paths by using the SAGE algorithm.

A. Delay Spread (DS)

It is noted that root mean square (rms) delay spread is defined as the square root of the second central moment of the power delay profile (PDP) normalized to the total power. The rms delay spread is defined as

$$\sigma_\tau = \sqrt{\frac{\sum_{n=1}^{N} P_D(\tau_n)(\tau_n - \bar{\tau})^2}{\sum_{n=1}^{N} P_D(\tau_n)}}$$

where N is number of multi-path, τ_n is the n-th delay estimated by the SAGE, $P_D(\tau)$ is the power delay spectrum and the mean delay $\bar{\tau}$ is obtained from

$$\bar{\tau} = \frac{\sum_{n=1}^{N} P_D(\tau_n)\tau_n}{\sum_{n=1}^{N} P_D(\tau_n)}$$

In this section, we evaluate the composite rms delay spread. This approach extends the view of a global delay spread of the channel environment. The rms delay spread reveals the frequency selectivity of the wideband channel, hence it is crucial in system design.

B. Circular Angle Spread (CAS)

To evaluate the spatial characteristics, the CAS is calculated as the square root second central moment of the power azimuth spectrum (PAS) due to the circular wrapping of the angles [5]. This CAS is constant regardless of the value of the angle shift. For the ASA and ASD analysis, we used the CAS method.

For a signal with N multi-paths, the CAS is defined as

Position	Office Scenario		
	DS [nsec]	ASA [°]	ASD [°]
LOS	18.57	72.23	59.78
NLOS	22.12	81.07	53.62

TABLE II
THE ESTIMATED LS PARAMETERS FOR BOTH LOS AND NLOS CONDITIONS

$$\sigma_{AS} = \min_{\Delta} \sigma_{AS}(\Delta) = \sqrt{\frac{\sum_{n=1}^{N} (\theta_{n,\mu}(\Delta))^2 \cdot P_n}{\sum_{n=1}^{N} P_n}}$$

where P_n is the power for the n-th path, and $\theta_{n,\mu}(\Delta)$ is defined as

$$\theta_{n,\mu}(\Delta) = \begin{cases} 2\pi + (\theta_n(\Delta) - \mu_\theta(\Delta)) & \text{if } (\theta_n(\Delta) - \mu_\theta(\Delta)) < \pi \\ (\theta_n(\Delta) - \mu_\theta(\Delta)) & \text{if } |(\theta_n(\Delta) - \mu_\theta(\Delta))| \geq \pi \\ 2\pi - (\theta_n(\Delta) - \mu_\theta(\Delta)) & \text{if } (\theta_n(\Delta) - \mu_\theta(\Delta)) > \pi \end{cases}$$

$\mu_\theta(\Delta)$ is defined as

$$\mu_\theta(\Delta) = \frac{\sum_{n=1}^{N} \theta_n(\Delta) \cdot P_n}{\sum_{n=1}^{N} P_n}$$

$$\theta_n(\Delta) = \theta_n + \Delta$$

where θ_n is the AoA or AoD of the n-th path estimated by the SAGE, and Δ denotes the angle shift ranging from $-\pi$ to π.

Fig. 5 shows cumulative distribution function (CDF) analysis results of DS and CAS at LOS and NLOS positions in the office scenario. Mean value of the LS parameters is summarized in the Table II. Most of the LS parameters in NLOS scenarios except the ASD have larger values than that in LOS scenarios. It indicates the fact that multi-paths go through more scatterings and reflections in NLOS scenarios.

C. Cross-Correlation between Large-scale Parameters

Cross-correlation was analyzed between the large-scale parameters. Fig. 6 depicts the LS parameters under LOS condition as a function of burst index. It also shows the LS parameters on the same time scale. It makes easier to see correlation between the parameters, although the exact values have not been given.

Mathematically, the cross-correlation is defined by

$$\rho_{xy} = \frac{C_{xy}}{\sqrt{C_{xx} C_{yy}}}$$

where C_{xy} is the cross-covariance of LS parameters x and y.

Table III summarize the estimated cross-correlations between the LS parameters. Comparing to the cross-correlation of the DS–ASD, 0.7, of the WINNER II channel model [6] in the indoor office scenario, it has been shown to yield good consistency. Although, in general correlation increases, there are some opposite cases, i.e. the cross-correlation between DS–ASA and ASA–ASD become -0.57 and -0.88, respectively. These results may be related to significantly lower LOS measurement data set. And even if in LOS scenarios, there are richer local scatterers around the Rx.

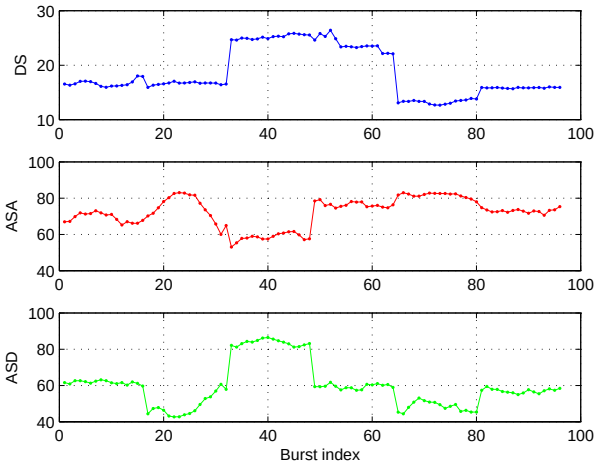

Fig. 6. LS parameters under LOS condition as a function of burst index

	Cross correlation
DS vs ASA	-0.57
DS vs ASD	0.76
ASA vs ASD	-0.88

TABLE III
THE ESTIMATED CROSS-CORRELATIONS BETWEEN LS PARAMETERS

D. Clustering of channel parameters

Many geometry-based stochastic channel models, such as SCM and WINNER II channel model use the concept of scattering clusters containing a number of stochastically varying multi-path components. One of the main problems of these models is the identification of multi-path clusters, hence to automatically identify clusters from measurement data and extract their characteristics. It has been investigated that multidimensional channel parameters obtained from MIMO measurements appear in clusters [7], i.e. in groups of multi-path components (MPCs) with similar parameters, such as delay, AoA and AoD.

Clustering was achieved by visual inspection, which gets very cumbersome for a large amount of measurement data. Recently, a scalable framework to automatically identify multi-path clusters was introduced [8], based on including power and the multi-path component distance (MCD) into the K-means concept. In this paper, we used the framework for the identification of the multi-path clusters except but the initialization step. The average linkage method which is the hierarchical clustering algorithm is used to initialize the cluster parameter estimates.

In a data post-processing step, estimated channel parameters were obtained by using the SAGE algorithm. Fig. 7(a) shows the unclustered indoor MIMO channel measurement data in

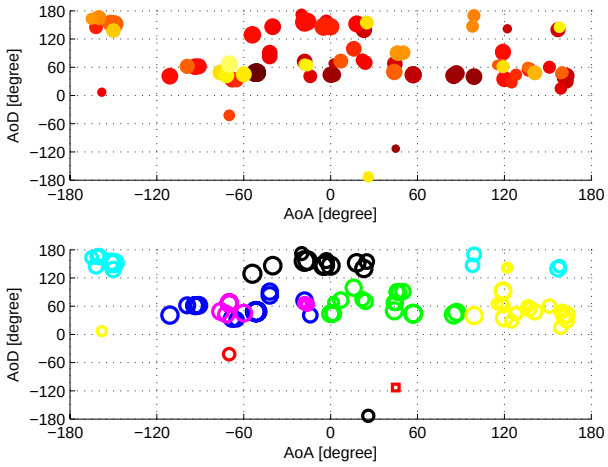

Fig. 7. Clustering results of the indoor office scenario

NLOS snapshot (Rx1), MPCs are color-coded with their delay and size of circles denotes their relative power. The clustering results are shown in Fig. 7(b). Same color and same shape denote a same cluster. In this snapshot, 8 clusters were identified. The obtained cluster parameter estimated are reported in Table IV.

The results demonstrate that the median value of the cluster number is 10 and 11 in LOS and NLOS scenarios, respectively.

CDF		10% percentile	50% percentile	90% percentile
Cluster Number	LOS	5	10	16
	NLOS	8	11	18
Cluster DS [nsec]	LOS	1.8	4.1	10.0
	NLOS	2.0	4.9	7.8
Cluster ASA [°]	LOS	6.6	13.2	22.0
	NLOS	5.8	11.1	17.9
Cluster ASD [°]	LOS	6.8	14.0	22.8
	NLOS	6.1	9.9	16.0

TABLE IV
PARAMETER ESTIMATES OF THE CLUSTERS IN THE INDOOR OFFICE SCENARIO

IV. CONCLUSIONS

The carrier frequency and the bandwidth will be up to 3.6 GHz and 100 MHz for the upcoming IMT-Advanced system. And interest of the wideband MIMO indoor channel model has been increased recently. In addition, an accurate characterization of the large-scale parameters is very important in design issues, especially for MIMO and broadband networks. Therefore we have performed measurement campaign for the wideband indoor office scenario using the BECS system at 3.7 GHz with 100 MHz RF bandwidth.

In this paper, we analyzed the large-scale parameters, such as delay spread and angular spread, based on the measured data in a typical indoor office. In addition, we presented cross-correlations between the large-scale parameters and clustering characteristics of multi-path components are also provided.

REFERENCES

[1] V. Erceg and *et al.*, "TGn Channel Models," *Doc. IEEE802.11-03/940r4*, 2004.
[2] G. Breit and *et al.*, "TGac Channel Model Addendum," *Doc. IEEE802.11-09/0308r10*, 2010.
[3] H. Chung, N. Vloeberghs, H. K. Kwon, S. J. Lee, and K. C. Lee, "MIMO channel sounder implementation and effects of sounder impairment on statistics of multipath delay spread," *Proc. IEEE VTC*, vol. 1, pp. 349–353, Sep. 2005.
[4] B. H. Fleury, M. Tschudin, R. Heddergott, D. Dahlhaus, and K. I. Pedersen, "Channel Parameter Estimation in Mobile Radio Environment Using the SAGE Algorithm," *IEEE Journal on Selected Areas in Communications*, vol. 17, pp. 434–450, Mar. 1999.
[5] 3GPP, "Spatial channel model for Multiple Input Multiple Output (MIMO) simulations," *TR 25.996 v6.1.0*, Sep. 2003.
[6] P. Kyosti and *et al.*, "WINNER II Channel Models," *IST-WINNER II D1.1.2*, Nov. 2007.
[7] D. L. S. M. M. B. C. C. Chong, C. M. Tan and A. Nix, "A new statistical wideband spatio-temporal channel model for 5-GHz band WLAN systems," *IEEE Journal on Selected Areas in Communications.*, vol. 21, pp. 139–150, Feb. 2003.
[8] J. S. E. B. J.-P. N. N. Czink, P. Cera and J. Ylitalo, "A framework for automatic clustering of parametric MIMO channel data including path powers," *IEEE Vehicular Technology Conference 2006 Fall*, Sep. 2006.